The Kinesin-8 Motor Kif18A Suppresses Kinetochore Movements to Control Mitotic Chromosome Alignment

Jason Stumpff,[1] George von Dassow,[2] Michael Wagenbach,[1] Charles Asbury,[1] and Linda Wordeman[1,*]
[1]Department of Physiology and Biophysics, University of Washington School of Medicine, Seattle, WA 98195, USA
[2]Center for Cell Dynamics, Friday Harbor Laboratories, University of Washington, Friday Harbor, WA 98250, USA
*Correspondence: worde@u.washington.edu
DOI 10.1016/j.devcel.2007.11.014

SUMMARY

During vertebrate cell division, chromosomes oscillate with periods of smooth motion interrupted by abrupt reversals in direction. These oscillations must be spatially constrained in order to align and segregate chromosomes with high fidelity, but the molecular mechanism for this activity is uncertain. We report here that the human kinesin-8 Kif18A has a primary role in the control of chromosome oscillations. Kif18A accumulates as a gradient on kinetochore microtubules in a manner dependent on its motor activity. Quantitative analyses of kinetochore movements reveal that Kif18A reduces the amplitude of preanaphase oscillations and slows poleward movement during anaphase. Thus, the microtubule-depolymerizing kinesin Kif18A has the unexpected function of suppressing chromosome movements. Based on these findings, we propose a molecular model in which Kif18A regulates kinetochore microtubule dynamics to control mitotic chromosome positioning.

INTRODUCTION

During mitosis, chromosomes establish connections to mitotic spindle microtubules (MTs) via specialized protein complexes called kinetochores, and subsequently translocate to the midzone of the bipolar spindle. This process, known as "congression," is essential for preserving the fidelity of the genome as it ensures that sister chromosomes will be segregated on either side of the cytokinetic furrow when it bisects the spindle midzone. Despite decades of study on this important process, the molecular mechanisms that allow chromosomes to find and remain at the spindle equator remain unclear.

Classic live imaging studies of congressing chromosomes established that bioriented chromosomes move at constant velocity and display abrupt changes in direction both before and after alignment (Rieder and Salmon, 1994; Skibbens et al., 1993). These oscillatory movements are surprisingly similar in unaligned and aligned chromosomes, with the exception that unaligned chromosomes tend to exhibit more directional persistence toward the center of the spindle between reversals (Skibbens et al., 1993). Current models for congression attempt to explain the decrease in directional persistence near the meta-

phase plate as a result of the combined influence of kinetochore-microtubule (kMT) dynamic instability and away-from-pole forces generated along chromosome arms by MTs and chromokinesins (i.e., polar ejection forces) (Joglekar and Hunt, 2002; Khodjakov et al., 1999; Rieder and Salmon, 1994). Whereas experimental evidence supports the idea that polar ejection forces vary with spindle position and thus could provide a positional cue (Ault et al., 1991; Cassimeris et al., 1994; Rieder et al., 1986; Rieder and Salmon, 1994), other data indicate that they are insufficient to explain congression (Kapoor and Compton, 2002). For example, abrogation of the polar ejection force via inhibition of chromokinesins does not abolish congression (Levesque and Compton, 2001). Furthermore, experimental removal of chromosome arms does not prevent kinetochores from aligning at the spindle equator (Brinkley et al., 1988). Taken together, these studies suggest that another mechanism, likely acting at kinetochores, provides spatial cues that are critical for alignment.

An alternative mechanism for congression revolves around an intriguing idea that kinetochores are "smart" and can sense their position within the spindle (Mitchison, 1989). In "smart" kinetochore models, the position-sensitive mechanism that determines when chromosomes change direction acts at kinetochores (Kapoor and Compton, 2002; Rieder and Salmon, 1994). Although molecular evidence to support a mechanism that would permit kinetochores to monitor their spindle position is lacking, the motor proteins of the kinesin-8 subfamily have the potential to fulfill such a role. In vitro studies have established that kinesin-8s are plus-end-directed motors that can depolymerize stable MTs specifically at their plus-ends in a length-dependent manner, suggesting a role in directly regulating MT dynamics and MT length in vivo (Gupta et al., 2006; Mayr et al., 2007; Pereira et al., 1997; Varga et al., 2006). Furthermore, genetic and siRNA-based studies indicate that kinesin-8 motors, including human Kif18A, are required for proper mitotic chromosome alignment (Gandhi et al., 2004; Garcia et al., 2002; Goshima and Vale, 2003; Mayr et al., 2007; West et al., 2002; Zhu et al., 2005). However, the question of how kinesin-8 motors functionally contribute to congression remains unanswered.

To investigate the mechanism by which Kif18A regulates chromosome congression, we have used high-resolution live cell imaging combined with quantitative measurements of kinetochore movements. We report that Kif18A controls the persistent movement of chromosomes by both increasing the rate at which they make directional switches and slowing the velocity of their movement. Furthermore, Kif18A's accumulation on kMTs and its ability to suppress oscillatory movements are dependent on its motor activity and vary within the spindle. Based on these

discoveries, we propose a model for chromosome congression in which Kif18A forms a gradient along kMTs that directly regulates their length and dynamics to facilitate chromosome alignment at the spindle equator.

RESULTS

Kif18A Forms a Motor-Dependent Gradient at kMT Plus-Ends

Endogenous Kif18A exhibits a dynamic localization to the plus-ends of kMTs (Figures 1A and 1B; see Figure S1 in the Supplemental Data available with this article online). The localization of Kif18A in mitotic HeLa cells was analyzed with anti-Kif18A antibodies and by expression of EGFP-Kif18A. Similar localization was observed with both approaches. In prometaphase cells, the motor is found along spindle MTs and localizes near the outer-kinetochore marker Hec1 at only a subset of kinetochores (Figures 1A–1D). In metaphase cells with aligned chromosomes, Kif18A localizes as a comet-like gradient along most if not all kMTs, and this localization requires Kif18A's motor activity (Figures 1A–1H; Figure S1). A mutant form of Kif18A (EGFP-Kif18A-mut), containing alanine substitutions in three conserved motor domain residues required for kinesin motility and kinesin-13 depolymerization (Moore et al., 2005; Woehlke et al., 1997), uniformly binds to spindle MTs and does not exhibit a gradient-like localization pattern (Figures 1E–1H). During anaphase, Kif18A is still seen at kinetochores and additionally begins to accumulate in the spindle midzone (Figure 1A; Figure S1). Kif18A concentrates at the midbody during telophase and cytokinesis (Figure S1).

Several additional features of Kif18A localization in metaphase cells were also observed. Analyses of metaphase sister kinetochore pairs coimmunostained with Hec1 and Kif18A antibodies revealed that the peak of Kif18A fluorescence is just distal to the peak of Hec1 fluorescence (Figure 1C), consistent with localization of Kif18A at kMT plus-ends. However, unlike Hec1 fluorescence, which is equal on both sister kinetochores, the peak intensity of Kif18A is significantly greater on one sister kinetochore relative to the other (Figures 1C and 1D). Analysis of optical sections through metaphase spindles revealed that the concentration of Kif18A, but not EGFP-Kif18A-mut, is greater on kMTs at the periphery of the spindle compared to those at the spindle interior closer to the pole-to-pole axis. Thus, the accumulation of Kif18A on kMT plus-ends varies within the spindle, and this differential accumulation is motor dependent (Figures 1E and 1F). Consistent with previous studies (Mayr et al., 2007), we found that Kif18A's localization to kinetochores was also dependent on MTs, as Kif18A was not detected at kinetochores after depolymerization of MTs with nocodazole or vinblastine (Figure S2). Taken together, these data suggest Kif18A utilizes its plus-end-directed motility to form a gradient along kMTs during metaphase and that accumulation is greater at the outer periphery of the spindle.

Kinetochore Oscillations Are Sensitive to Alterations in Kif18A Expression

To address Kif18A's role during chromosome congression, cells were either depleted of Kif18A by siRNA treatment or transfected with EGFP-Kif18A to increase Kif18A expression. Treatment with Kif18A-specific siRNAs resulted in the depletion of Kif18A from mitotic spindles and kinetochores (Figure S3). The amount of Kif18A that remained after siRNA depletion was below the level of detection for our antibody (>90% depletion; Figure S3C). Consistent with previous reports (Mayr et al., 2007; Zhu et al., 2005), we observed that depletion of Kif18A resulted in failed chromosome alignment (Figures S3A and S3B) and an increase in prometaphase cells (Figure S3D). In contrast, expression of EGFP-Kif18A did not cause a mitotic delay or disrupt chromosome alignment (Figure S3D).

To address a role for Kif18A in regulating mitotic chromosome movements, HeLa cells coexpressing fluorescent kinetochore and centrosome markers were analyzed by time-lapse microscopy following transfection with siRNAs or EGFP-Kif18A. We observed that chromosomes in these cells were bioriented and made oscillatory movements around the equator of the spindle reminiscent of those observed in late prometaphase and metaphase control cells (Figures 2A–2C; Movies S1–S3). Bioriented kinetochores in these cells were also under tension, as determined by measuring the distance between sister kinetochores over time. Whereas distributions of interkinetochore distance were similar in all cell types tested, alterations in Kif18A levels correlated with small but significant changes in the average interkinetochore distance (Figure 2D). Kif18A depletion reduced the average interkinetochore distance, consistent with previous measurements in fixed cells (Mayr et al., 2007; Zhu et al., 2005), whereas EGFP-Kif18A expression led to greater interkinetochore distance. However, the most striking effects induced by altering Kif18A expression were changes in oscillation amplitude. Oscillatory movements were dramatically increased in the absence of Kif18A and were suppressed in EGFP-Kif18A cells. These effects are evident in plots of individual kinetochore movements relative to spindle poles (Figure 2A) and in kymographs generated from CENP-B fluorescence (Figure 2C).

In order to quantify changes in oscillatory movement in a population of kinetochores, we developed a measurement that scores the deviation from the average position (DAP) for individually tracked bioriented kinetochores. The DAP for a kinetochore is a linear measure of oscillation amplitude that provides a means to quantitatively analyze kinetochore movements even when unambiguous determination of directional changes is difficult, such as in the suppressed oscillations observed in EGFP-Kif18A cells (for more information, see Figure S4). These studies revealed that depletion of Kif18A significantly increased the DAP from 0.46 ± 0.02 μm to 0.85 ± 0.03 μm, whereas overexpression of Kif18A significantly reduced the DAP to 0.31 ± 0.01 μm (Figure 2E; Table 1). Therefore, the distance that kinetochores move from their average position during oscillations is increased approximately 2-fold in the absence of Kif18A and is reduced by approximately 30% in the presence of EGFP-Kif18A. Furthermore, the suppression of oscillatory movements is dependent on Kif18A's motor activity, as expression of EGFP-Kif18A-mut did not affect oscillations (Figures 2A–2C and 2E). These data indicate that Kif18A limits persistent movement of bioriented kinetochores in a motor-dependent fashion and that increased oscillation amplitude is likely the primary defect that leads to the unaligned chromosome phenotype seen in Kif18A-depleted cells.
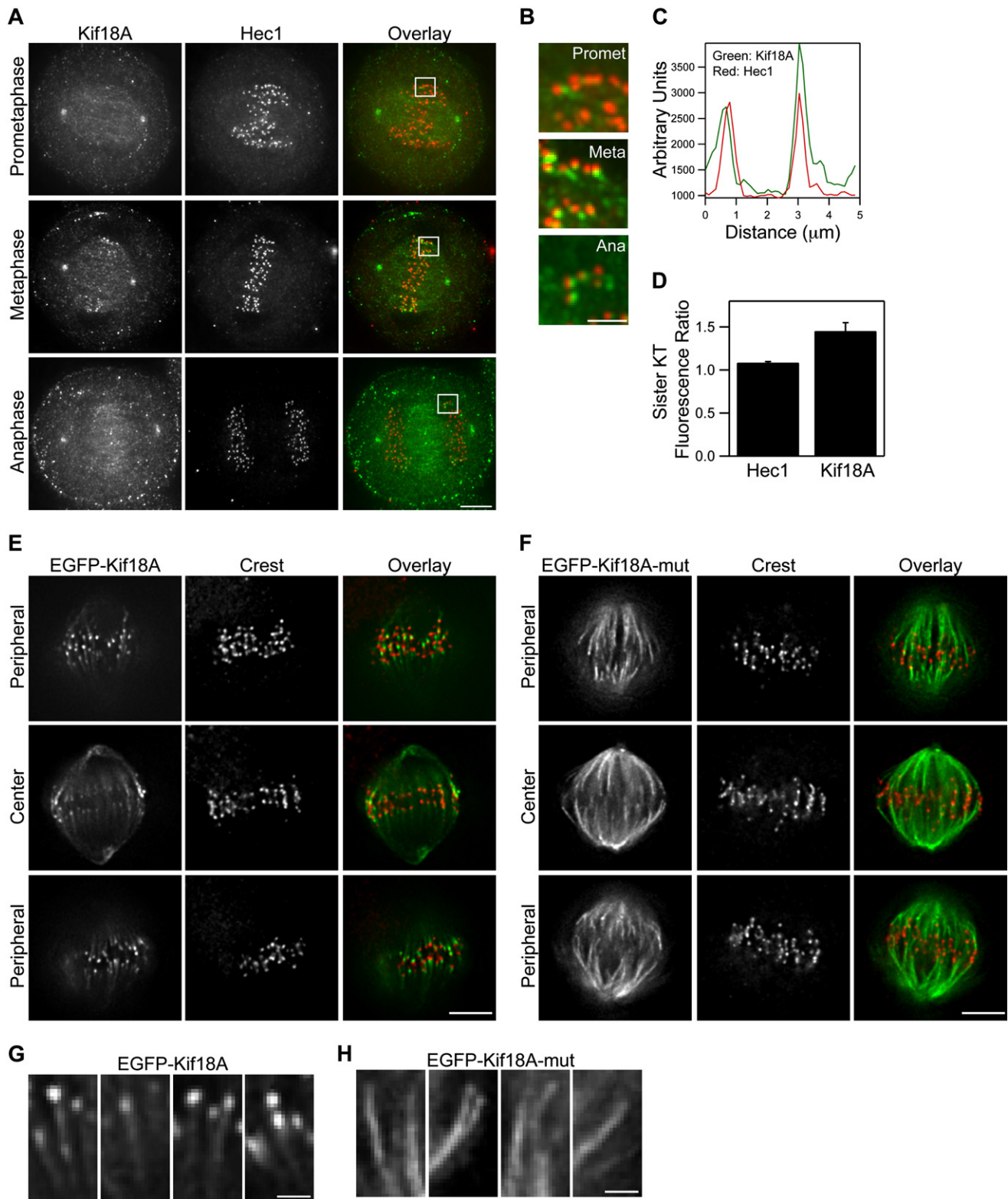
Figure 1. Kif18A Displays Dynamic, Motor-Dependent Localization to the Plus-Ends of Kinetochore Microtubules

(A) Mitotic HeLa cells in the indicated stages were fixed and stained with anti-Kif18A antibodies (green in overlay) and anti-Hec1 antibodies (red in overlay). Scale bar represents 5 μm.

(B) Magnified views of the regions indicated by white boxes in prometaphase (promet), metaphase (meta), and anaphase (ana) cells in (A). Scale bar represents 2 μm.

In addition to suppressing oscillations, we observed that EGFP-Kif18A expression often led to uncoordinated sister kinetochore movements. Specifically, one kinetochore frequently attempted to move poleward while its sister remained stationary or also attempted poleward movement (see Movie S3). The transient increases in interkinetochore distance caused by these events are evident in our distribution of measurements as a shoulder above 1 μm and might explain the increase in average interkinetochore distance induced specifically by EGFP-Kif18A but not EGFP-Kif18A-mut expression (Figure 2D).

Oscillation Amplitude Correlates with Kif18A Accumulation at Kinetochores

Because the concentration of Kif18A is higher on kMTs at the periphery of the spindle compared to those nearer to the pole-to-pole axis (Figure 1E), we compared oscillatory movements of kinetochores based on their location within the spindle. In control siRNA-treated cells, we found that oscillations of peripheral kinetochores were significantly reduced compared to those of kinetochores closer to the long axis of the spindle (Figure 2F), consistent with previous studies in PtK1 cells (Canman et al., 2002; Cimini et al., 2004). Depletion of Kif18A significantly increased the movements of peripheral and internal kinetochores, suggesting that Kif18A limits oscillatory movements of all kinetochores (Figure 2F). Interestingly, we also found that oscillations of peripheral and internal kinetochores were not significantly different in EGFP-Kif18A cells and that oscillations in these cells are comparable to those of peripheral kinetochores in control cells (Figure 2F). These data show that oscillation amplitude is inversely correlated with the concentration of Kif18A on kMTs.

The Effects of Kif18A on Chromosome Oscillations Are Not a Result of Changes in Spindle Length

Consistent with studies in fixed cells (Mayr et al., 2007), we found that spindles in live cells depleted of Kif18A are longer on average than control spindles (Figures 3A and 3B). Polar ejection forces generated by each half-spindle are believed to play a significant role in the regulation of chromosome oscillations during mitosis by generating away-from-pole forces along chromosome arms, which increase as chromosomes enter MT-dense regions near centrosomes (Cassimeris et al., 1994; Rieder et al., 1986; Rieder and Salmon, 1994). In principle, an increase in spindle length could indirectly lead to larger chromosome oscillations by positioning areas of MT density farther from the spindle equator. However, analysis of kinetochore oscillations as a function of spindle length does not support this hypothesis (Figure 3C). Within a cell population there is little correlation between spindle length and oscillation amplitude. Furthermore, when oscillatory movements in control and Kif18A-depleted cells with spindles of similar length are compared (between 15

and 17 μm), oscillations are larger in the absence of Kif18A (Figure 3C). These data indicate that the effects of Kif18A on chromosome oscillations are not simply an indirect effect of changes in spindle length and suggest a direct role for Kif18A in controlling chromosome movements.

Kif18A Affects the Velocity and Switch Rate of Kinetochore Movements

Oscillation amplitude could be affected by alterations in two independent characteristics of chromosome movement: velocity and the frequency of directional switches. To calculate the switch rate for a kinetochore, we counted the number of times it changed directions during oscillatory movement and divided that number by the amount of time the kinetochore was filmed. On average, the kinetochore switch rate is reduced in cells depleted of Kif18A compared to controls (Figure 4A; Table 1). Kinetochores in control-depleted cells changed direction at an average rate of 1.58 ± 0.05 min^{-1}, whereas those in Kif18A-depleted cells switched direction at an average rate of 1.23 ± 0.11 min^{-1}. These data suggest that kinetochores in Kif18A-depleted cells undergo longer periods of persistent movement between turnarounds.

The velocity of oscillatory movements was also significantly increased in Kif18A-depleted cells relative to controls (Figure 4B; Table 1). Kinetochores in control-depleted cells moved at an average rate of 1.92 ± 0.06 μm/min, whereas those in Kif18A-depleted cells oscillated at an average rate of 2.80 ± 0.08 μm/min. Furthermore, poleward and away-from-pole movements were equally affected (Figure 4B; Table 1). The increase in velocity in the absence of Kif18A is surprising, because it implies that Kif18A, an MT depolymerizer, acts to slow chromosome movement in vivo. In contrast to our findings, another study reported that Kif18A depletion reduces the velocity of kinetochore movements (Mayr et al., 2007). The exact reason for these conflicting results is not clear, but we feel that the differences might be a result of the use of low time resolution in the previous study, which would prevent accurate determination of directional chromosome speeds (see Experimental Procedures).

Our data indicate that both an increase in velocity and a decrease in directional switch frequency lead to a 2-fold increase in oscillation amplitude from 1.21 ± 0.08 μm to 2.28 ± 0.15 μm in Kif18A-depleted cells, consistent with the observed 2-fold change in DAP (Table 1). Thus, a combination of changes in switch rate and velocity quantitatively explains the increased movements observed in Kif18A-depleted cells.

Kif18A Affects the Velocity of Poleward Anaphase Movements

Because Kif18A is also present on kinetochores in anaphase cells (Figure 1A), we tested whether Kif18A affects the velocity

---

(C) Representative linescan across metaphase sister kinetochores in a HeLa cell stained with anti-Kif18A (green) and anti-Hec1 (red) antibodies. In all scans, the peak of Kif18A fluorescence was distal to the peak of Hec1 fluorescence with respect to the centromere (n = 19 kinetochore pairs from three cells).

(D) The ratio of peak fluorescence intensity on sister kinetochores was calculated from metaphase cells costained for Hec1 and Kif18A by immunofluorescence. The peak intensity of Hec1 is equal between sister kinetochores, whereas Kif18A is significantly higher on one sister kinetochore than the other (n = 19 kinetochore pairs from three cells; p = 0.001). Error bars indicate SEM.

(E and F) Metaphase HeLa cells expressing either EGFP-Kif18A (E) or EGFP-Kif18A mutant (F) (green in overlay) and stained with human CREST serum to visualize kinetochores (red in overlay). Optical slices from the periphery and the center of each spindle are displayed. Scale bars represent 5 μm.

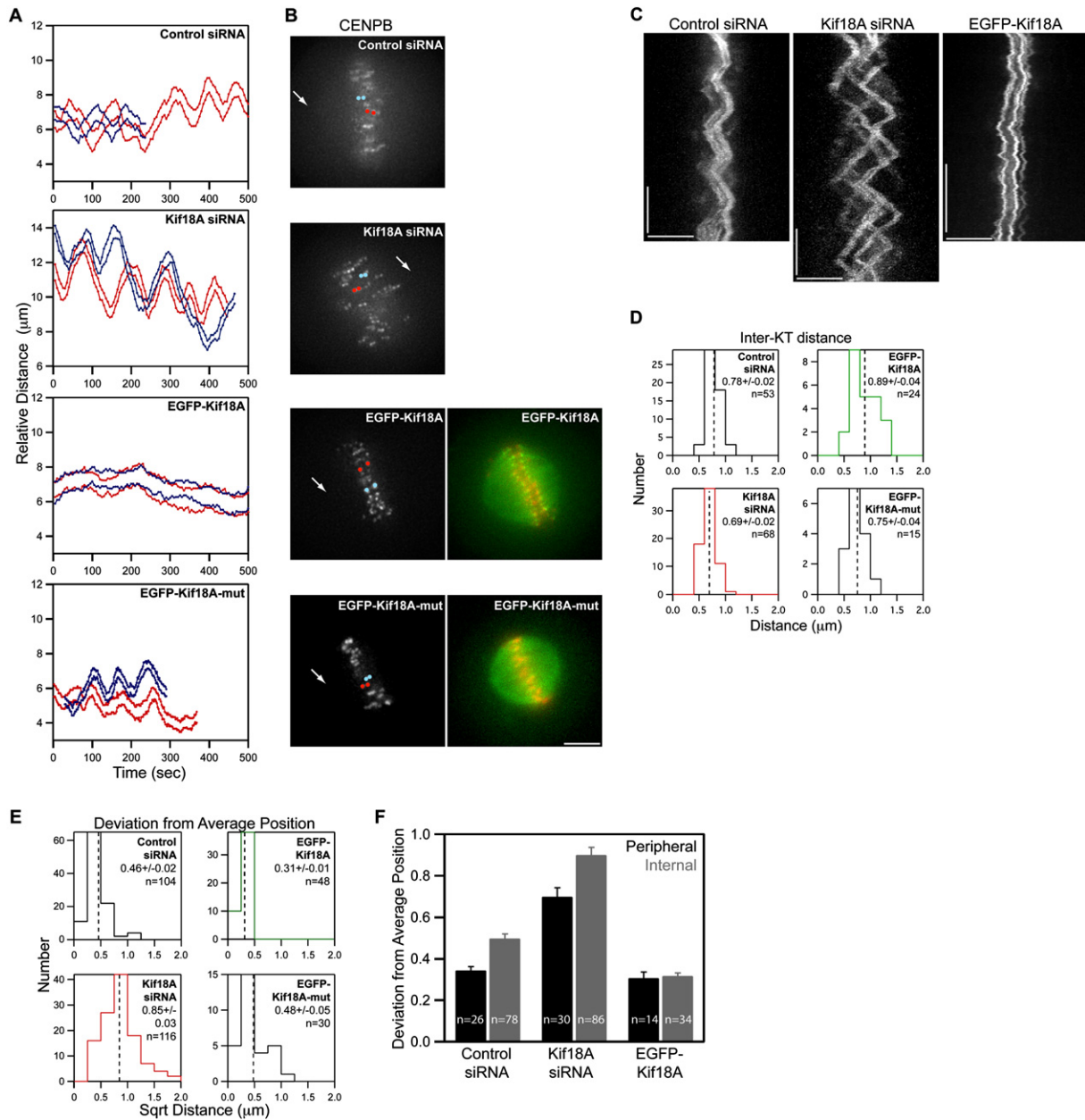(G and H) Magnified images of EGFP-Kif18A (G) or EGFP-Kif18A-mut (H) along kMTs. Scale bars represent 1 μm.

Figure 2. Kif18A Affects the Oscillatory Movements of Kinetochores

(A) Distance versus time plots of two kinetochore pairs (red and blue lines) from each of the indicated cell types. Relative distance was calculated by measuring the separation between each kinetochore and one spindle pole. Images were collected every 5 s for control and Kif18A siRNA cells and every 2 s for EGFP-Kif18A and EGFP-Kif18A-mut cells.

(B) Still frames of CENP-B fluorescence in cells used to derive the distance versus time plots shown in (A). Arrows indicate position of pole used for relative distance measurements. Red and blue dots are overlayed on kinetochores that were tracked to generate the red and blue traces in (A), respectively. Two-color images of EGFP-Kif18A or EGFP-Kif18A-mut (green) with mRFP-CENP-B (red) were taken immediately after time-lapse imaging of kinetochore movements was stopped. Scale bar represents 5 μm.

(C) Representative kymographs of CENP-B fluorescence from cells transfected with control siRNAs, Kif18A-specific siRNAs, or EGFP-Kif18A. Vertical scale bars represent 2 min; horizontal scale bars represent 5 μm.

(D) Histograms displaying average interkinetochore distances for sister kinetochore pairs in live cells. The mean ± SEM is indicated for each distribution and the mean position is marked by a vertical dotted line. "n" indicates the number of kinetochore pairs tracked from ten (control and Kif18A siRNA), seven (EGFP-Kif18A), or four (EGFP-Kif18A-mut) cells. The average interkinetochore distances measured from Kif18A siRNA and EGFP-Kif18A-expressing cells are significantly different from those measured in control siRNA-treated cells (p = 1.0×10^{-4} and p = 0.02, respectively). Average interkinetochore distances for EGFP-Kif18A-expressing cells are also significantly different from EGFP-Kif18A-mut-expressing cells (p = 0.02).

(E) Histograms displaying deviation from average position (DAP) calculations for the indicated cell types. The mean ± SEM is given for each distribution and the mean position is marked by a vertical dotted line. "n" indicates the number of kinetochores analyzed from the same data set used in (D). The DAPs for

Table 1. Measurements of Preanaphase Kinetochore Movements

	P Vel (μm min^{-1})	AP Vel (μm min^{-1})	Switch (min^{-1})	Amp (μm)	DAP (μm)	IKD (μm)
Control siRNA	1.99 ± 0.07	1.81 ± 0.07	1.58 ± 0.05	1.21 ± 0.08	0.46 ± 0.02	0.78 ± 0.02
Kif18A siRNA	2.97 ± 0.09**	2.67 ± 0.08**	1.23 ± 0.11**	2.28 ± 0.15**	0.85 ± 0.03**	0.69 ± 0.02**
EGFP-Kif18A	ND	ND	ND	ND	0.31 ± 0.01**	0.89 ± 0.04*
EGFP-Kif18A-mut	ND	ND	ND	ND	0.48 ± 0.05	0.75 ± 0.04

Average measurements of poleward velocity (P Vel), away-from-pole velocity (AP vel), switch rate (Switch), oscillation amplitude (Amp), deviation from average position (DAP), and interkinetochore distance (IKD) are given ± SEM. *$p \leq 0.05$ and **$p \leq 0.01$ compared to controls. ND, not determined.

of poleward chromosome movements during anaphase. Depletion of Kif18A results in a mitotic delay mediated by the spindle assembly checkpoint, and very few Kif18A-depleted cells go through anaphase (Mayr et al., 2007; Zhu et al., 2005) (Figure S3D). Kif18A-depleted cells, however, are able to progress through anaphase, and exit mitosis when the checkpoint protein Mad2 is simultaneously depleted (Mayr et al., 2007) (Figure S3D). Therefore, we analyzed anaphase kinetochore movements in cells codepleted of Mad2 and Kif18A. Consistent with previous studies, Mad2-depleted cells entered anaphase before completing congression (Canman et al., 2002; Meraldi et al., 2004). Although most kinetochores segregated to the spindle poles normally, lagging chromosomes were frequently seen in cells depleted of Mad2 alone or codepleted of Mad2 and Kif18A (Figure 5A; see Movies S4 and S5). Anaphase A rates for nonlagging chromosomes increased approximately 20% from 1.68 ± 0.08 μm/min to 2.12 ± 0.14 μm/min in the absence of Kif18A (Figure 5B). However, we observed that loss of Kif18A function did not affect all kinetochores equally under these conditions and that only a subset of kinetochores in Mad2/Kif18A-depleted cells moved faster than controls. This could be a result of the increased frequency of merotelic attachments seen when cells are induced to enter anaphase precociously (Cimini et al., 2003).

To further investigate Kif18A's effects on anaphase kinetochore movements, we analyzed the small fraction of Kif18A siRNA-treated cells that happened to enter anaphase without checkpoint knockdown. For these studies, we chose cells with large preanaphase oscillations that initiated chromosome segregation without completing alignment, which are indications of Kif18A depletion. The average kinetochore poleward velocity in these cells was increased by approximately 40% to 2.83 ± 0.15 μm/min and, importantly, the majority of kinetochores displayed increased speed relative to controls (Figure 5B; Movies S6 and S7). In contrast, expression of EGFP-Kif18A slowed anaphase A velocity by approximately 45% to 0.92 ± 0.04 μm/min (Figure 5B; Movie S8). Taken together, these results suggest that Kif18A acts as a governor to limit the rate of kinetochore movements during mitosis, a function that is quite unexpected considering its MT depolymerization activity in vitro (Mayr et al., 2007).

DISCUSSION

Metaphase chromosomes in vertebrate cells make oscillatory movements around the spindle equator, and the regulation of these movements is believed to be important for establishing and maintaining alignment (Kapoor and Compton, 2002; Rieder and Salmon, 1994; Skibbens et al., 1993). Our data indicate that Kif18A functions to limit these oscillatory movements and control chromosome alignment.

We show that during mitosis, Kif18A suppresses the amplitude of kinetochore oscillations in part by increasing the rate at which kinetochores change directions. Kinetochore movements in vertebrate cells are thought to depend primarily on kMT plus-end dynamics (Inoue and Salmon, 1995; Rieder and Salmon, 1994). Kif18A's localization to kMT plus-ends and its in vitro MT depolymerizing activity suggest that it might directly modulate chromosome movements (Mayr et al., 2007). Directional switching involves both catastrophe and rescue of kMT plus-ends. Interestingly, Kip3p increases both the rescue and catastrophe frequencies of MTs in budding yeast (Gupta et al., 2006). A similar effect during mitosis would increase the frequency and suppress the amplitude of kinetochore oscillations, as we observed.

Kif18A-mediated changes in kinetochore oscillation amplitude were also due in part to a surprising and counterintuitive effect on the velocity of chromosome movements. In the absence of Kif18A, kinetochore velocity was increased during preanaphase oscillations and anaphase. Conversely, overexpression of Kif18A slowed poleward anaphase movements. These data indicate that Kif18A functions to slow kinetochore velocity and, importantly, argue against the previously suggested idea that Kif18A produces the force that drives chromosome movements (Mayr et al., 2007).

Exactly how Kif18A affects kinetochore velocity is an interesting question that warrants further investigation. One possible explanation for the observed effects on kinetochore velocity is suggested by recent studies of the *Drosophila* kinesin-8 motor Klp67A (Buster et al., 2007). In the absence of Klp67A, the rate of kMT flux, and thus the rate of kMT minus-end shortening, is increased, which leads to faster anaphase poleward movement. However, it is unclear whether changes in flux rate can fully explain the dramatic effects of altering Kif18A expression in human

kinetochores in Kif18A-depleted cells and EGFP-Kif18A cells are significantly different from the DAP for kinetochores in control siRNA cells (p = 4.4 × 10^{-22} and 1.2 × 10^{-9}, respectively). The DAP for EGFP-Kif18A kinetochores is also significantly different from the DAP for EGFP-Kif18A-mut kinetochores (p = 0.002). (F) Average DAP measurements for kinetochores on the periphery of the spindle (peripheral) and along the pole-to-pole axis (internal) from cells treated with control or Kif18A siRNAs or overexpressing EGFP-Kif18A. Error bars are SEM. "n" indicates the number of kinetochores from the data set used in (E). DAPs for peripheral and internal kinetochores are significantly different in control- and Kif18A-depleted cells (p = 5.9 × 10^{-7} and p = 7.0 × 10^{-4}, respectively) but not in EGFP-Kif18A cells (p = 0.75).
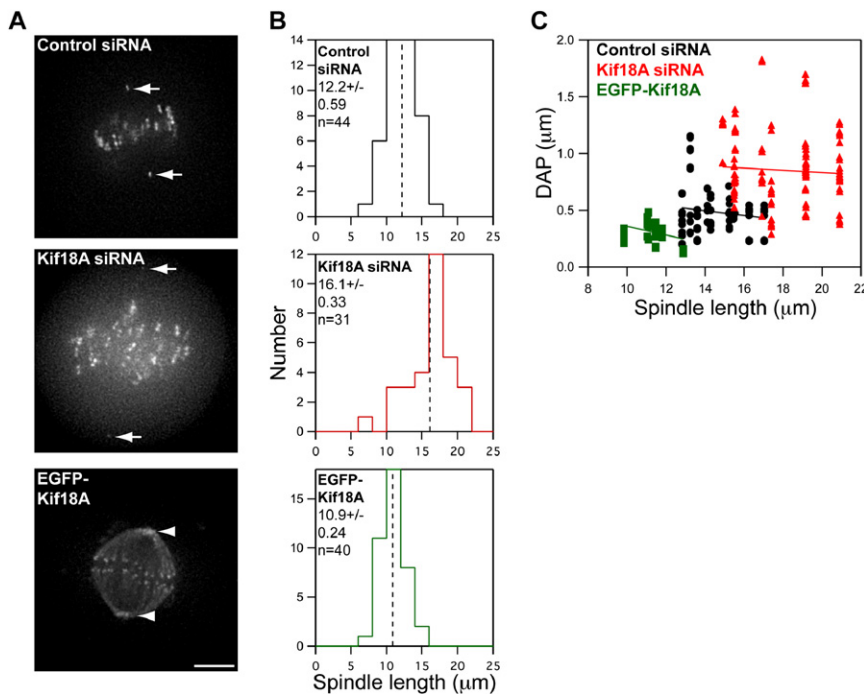
Figure 3. Kif18A's Effects on Oscillations Are Not an Indirect Effect of Changes in Spindle Length

(A) Images of live HeLa cells expressing Venus-centrin and EGFP-CENP-B (control and Kif18A siRNA) or EGFP-Kif18A. Spindle lengths were determined by measuring the distance between Venus-centrin foci (arrows) or EGFP-Kif18A spindle pole labeling (arrowheads). Scale bar represents 5 μm.

(B) Histograms of spindle lengths measured in live cells. The mean ± SEM is given for each distribution and the mean position is marked by a vertical dotted line. "n" indicates the number of cells analyzed. Spindle lengths in Kif18A-depleted and EGFP-Kif18A-expressing cells are significantly different from those in control-depleted cells ($p = 4.4 \times 10^{-7}$ and $p = 0.002$, respectively).

(C) Scatter plot of deviation from average position (DAP) measurements as a function of spindle length. Black circles, control siRNA; red triangles, Kif18A siRNA; green squares, EGFP-Kif18A. Lines represent regression fits to each data set.

cells, where flux makes only a minor contribution to the movement and alignment of chromosomes (Ganem and Compton, 2006). For example, flux in human cells accounts for 20% of chromosome poleward velocity (Ganem et al., 2005), so even if Kif18A overexpression completely suppressed flux, it would not be enough to explain the 45% decrease in velocity that we observed. Alternatively, Kif18A's accumulation at the plus-ends of kMTs might affect the kinetics of tubulin addition and release. The measured effects of kinesin-8 motors on MT dynamics and chromosome movements in yeast, where MTs do not flux, support this hypothesis (Garcia et al., 2002; Gupta et al., 2006; Maddox et al., 2000; Mallavarapu et al., 1999; Pearson et al., 2003; West et al., 2002). Thus, based on current data, we favor a model in which Kif18A affects kinetochore velocity through regulation of kMT plus-end dynamics, although effects on minus-end dynamics cannot be ruled out. Future work aimed at determining whether and how kinesin-8 motors directly modulate MT dynamics should help resolve this question.

Our studies also reveal that Kif18A forms a gradient on kMTs that is dependent on its motor activity, suggesting that Kif18A's plus-end-directed motility is required for the concentration of the motor at the plus-ends of kMTs. Interestingly, the extent of Kif18A's accumulation at kMT plus-ends varies within the spindle, as it is more concentrated on kMTs at the spindle periphery. The absolute concentration of motor could be influenced by a variety of factors such as length, stability, or numbers of MTs within the kinetochore fiber. Interestingly, studies of purified Kip3p reveal that its rate of in vitro depolymerization is proportional to MT length, which is correlated with the accumulation of a higher concentration of the motor at the plus-ends (Varga et al., 2006). This leads us to propose a model wherein Kif18A utilizes a combination of length-dependent plus-end accumulation and concentration-dependent modulation of kMT plus-end dynamics to control mitotic chromosome positioning. In our model, Kif18A protein

will accumulate at the plus-end of a kMT as it lengthens beyond the midzone (the center of the graph in Figure 6), and will dissociate as the kMT shortens. Our observation that the concentration of Kif18A is higher on one sister kinetochore than the other is consistent with this idea. As Kif18A accumulates at the plus-end, it increases to a threshold beyond which the probability that a kMT will undergo catastrophe is high, and in turn increases the chance that a chromosome will switch from away-from-pole to poleward movement. Such a mechanism would limit persistent movement and restrict oscillations of bioriented chromosomes to a region around the spindle equator where kMTs connected to opposite spindle poles are of relatively equal length (Figure 6).

This model, in which Kif18A regulates kMT plus-ends in a concentration-dependent manner, is consistent with our analyses of kinetochore movements. We observed that increasing the concentration of Kif18A in the cell leads to both an increase in the accumulation of Kif18A at kMT plus-ends and a reduction in oscillation amplitude (Figure 6). In this situation, kinetochores have relatively high levels of Kif18A the majority of the time, and thus kMTs might be strongly biased toward shortening. This, in turn, could cause sister kinetochores on bioriented chromosomes to initiate poleward movement simultaneously, reducing coordinated sister chromosome movement and transiently increasing interkinetochore distance as we observed when Kif18A was overexpressed. In contrast, decreasing Kif18A leads to larger kinetochore oscillations, perhaps by preventing threshold accumulation of Kif18A at kMT plus-ends (Figure 6). Quantitatively, however, oscillation amplitude does not seem to be solely dependent on Kif18A concentration because near-complete depletion of the protein does not completely randomize chromosome distribution (e.g., >90% depletion only increases oscillation amplitude 2-fold). Therefore, other cues, such as polar ejection forces or tension-dependent mechanisms, might be acting in parallel.
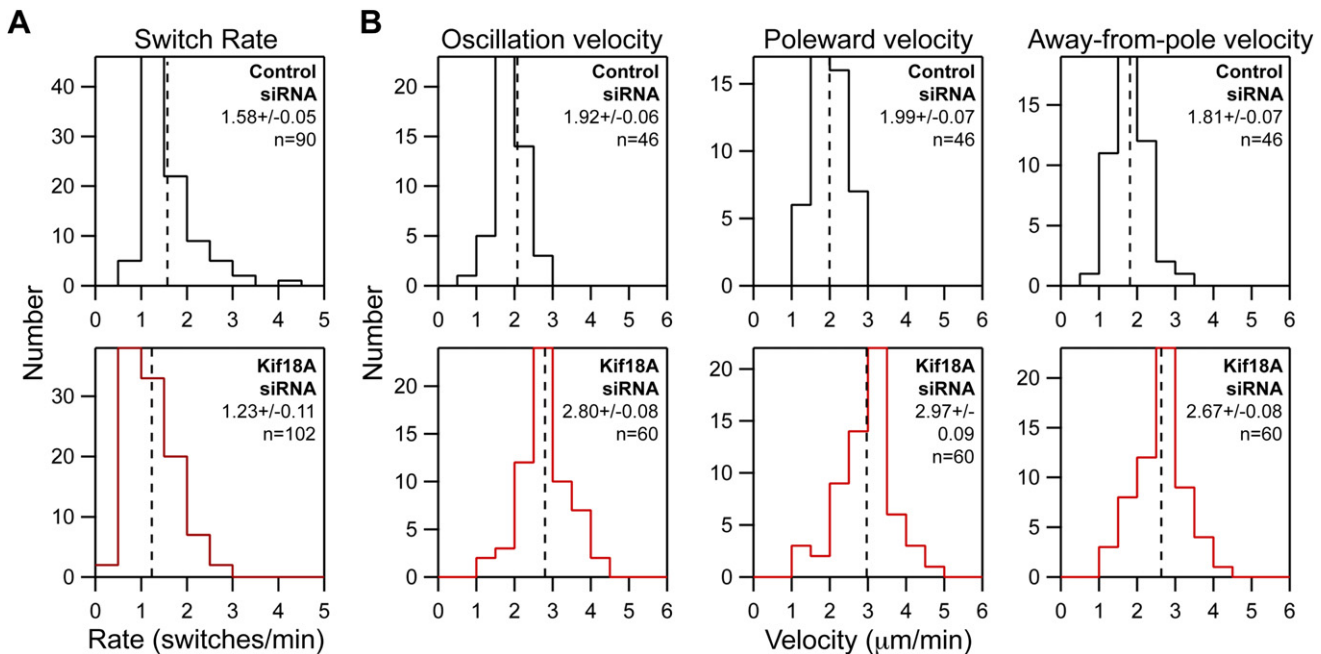
Figure 4. Kif18A Regulates Both the Directional Switch Rate and Velocity of Kinetochore Oscillations

(A) Histograms showing the distribution of kinetochore directional switch rates measured in control and Kif18A siRNA cells. The mean ± SEM is given for each distribution and the mean position is marked by a vertical dotted line. An average switch rate was calculated for each kinetochore and "n" indicates the number of kinetochores analyzed from ten control and ten Kif18A siRNA cells. The two data sets are significantly different (p = 2.8 × 10^{-5}).

(B) Histograms of average kinetochore velocities during oscillatory movements in control- and Kif18A siRNA-treated cells. The oscillation velocity distribution displays the average velocity for each kinetochore analyzed. Poleward velocity and away-from-pole velocity distributions include only velocities from movements made toward or away from the pole that the kinetochore was attached to, respectively. The mean ± SEM is given for each distribution and the mean position is marked by a vertical dotted line. "n" indicates the number of kinetochores analyzed from five control and five Kif18A siRNA cells. Kinetochore velocities in Kif18A-depleted cells are significantly different from those in control-depleted cells (p = 2.8 × 10^{-15} for average oscillation velocity; p = 5.4 × 10^{-13} for poleward velocity; p = 4.2 × 10^{-12} for away-from-pole velocity).

The correlation between Kif18A's localization and kinetochore oscillations in control cells is also consistent with this model. Kif18A accumulates to a greater extent on the kMTs at the periphery of the spindle, and the oscillations of peripheral kinetochores are reduced compared to those attached to kMTs along the pole-to-pole axis. This phenomenon is not specific to HeLa cells, as similar variations in kinetochore movements have been observed in PtK1 cells (Canman et al., 2002; Cimini et al., 2004). Interestingly, increasing the concentration of Kif18A in the cell suppresses all kinetochore movements to the level seen at the spindle periphery in control cells. The fact that increased Kif18A does not further limit peripheral chromosome movements suggests that endogenous Kif18A already suppresses chromosome movements maximally at the spindle periphery in control cells.

In conclusion, our data suggest a model in which length-dependent modulation of kMT dynamics by Kif18A provides a spatial cue to control chromosome oscillations and thereby facilitate accurate organization and segregation of chromosomes during cell division.

EXPERIMENTAL PROCEDURES

Cell Culture and Transfections

HeLa cells were cultured as previously described (Maney et al., 1998). HeLa cells were transfected with plasmid DNA by electroporation using Nucleofec-

tor II (Amaxa) according to the manufacturer's instructions. Cells were transfected with siRNA using oligofectamine transfection reagent (Invitrogen) according to the manufacturer's instructions. For Kif18A depletion, cells were transfected with 60 nM each siRNAs targeting the Kif18A sequences 5′-GCCAAUUCUUCGUAGUUUU-3′ and 5′-GCAGCUGGAUUUCAUAAA-3′ (Ambion). Treatment with this combination of siRNAs or with either siRNA alone at 120 nM produced indistinguishable effects. For Mad2 depletion, cells were transfected with 60 nM each siRNAs targeting the sequences 5′-GGAUGAC AUGAGGAAAAUA-3′ and 5′-GCGUGGCAUAUAUCCAUCU-3′ (Ambion). For control depletions, cells were transfected with 120 nM (for Kif18A single-knockdown experiments) or 240 nM (for Kif18A/Mad2 double-knockdown experiments) negative control siRNA 1 (Ambion). Control siRNA treatment did not alter chromosome alignment or kinetochore movements relative to untreated control cells (data not shown).

Construction of DNA Plasmids

EGFP-CENP-B (pGFPCPB1) was constructed by PCR amplification of codons 1–167 of the *Cricetulus griseus* CENP-B gene (a kind gift from Manuel Valdivia, University of Cadiz, Spain) and subcloning into the EcoRI and XbaI sites of pEGFP-C1 (Clontech). To prepare mRFP-CENP-B (pMX234), the EGFP gene of pEGFP-N1 (Clontech) was replaced by PCR-amplified mRFP1.0 (Campbell et al., 2002) and codons 1–167 of CENP-B to generate an EcoRI-Not1 fragment bearing the mRFP-CENP-B fusion. EGFP-Kif18A was constructed by PCR amplification of codons 1–898 of the human Kif18A gene and subcloning into the EcoRI and Not1 sites of pEGFP-C1 (Clontech). Site-directed mutagenesis was used to change H304, R308, and K311 to alanine in the EGFP-Kif18A mutant. Venus-centrin was a kind gift from Benjamin Major and Randall Moon.
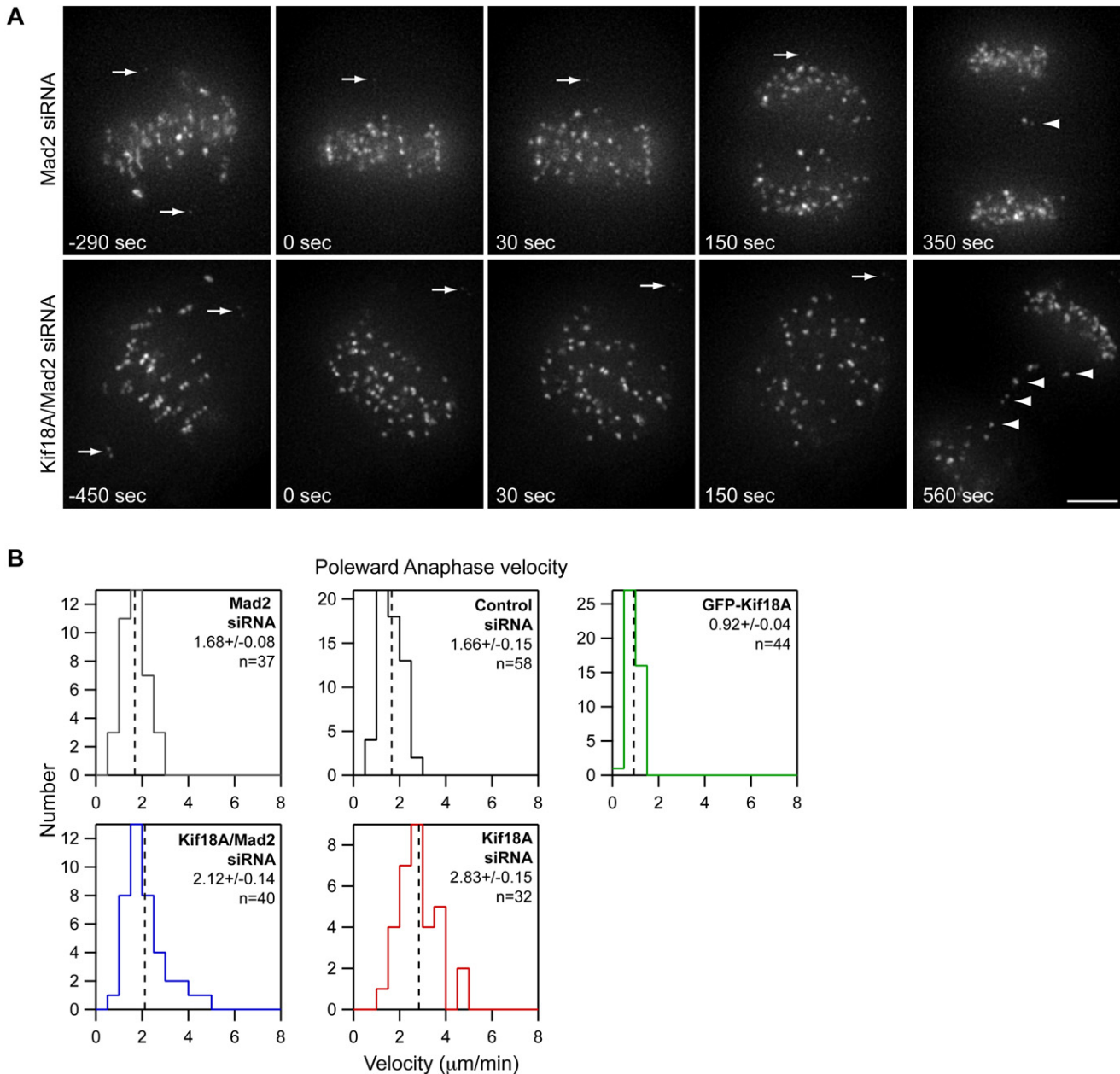
Figure 5. Kif18A Affects Poleward Movement during Anaphase

(A) Selected images from time-lapse analyses of Mad2-depleted and Kif18A/Mad2-codepleted HeLa cells expressing EGFP-CENP-B and Venus-centrin. Time is given in seconds relative to anaphase sister kinetochore separation. Arrows mark the position of Venus-centrin-labeled spindle poles. In both cells, the lower spindle pole is out of focus at the time of anaphase. Kinetochores on lagging chromosomes are marked by arrowheads. Cells were filmed at 5 s intervals. Scale bar represents 5 μm.

(B) Histograms of anaphase A velocities measured in control siRNA, Mad2 siRNA, Kif18A/Mad2 siRNA, Kif18A siRNA, and EGFP-Kif18A cells. The mean ± SEM is given for each distribution and the mean position is marked by a vertical dotted line. "n" indicates the number of kinetochores analyzed from three cells (Kif18A siRNA, Mad2 siRNA, and Kif18A/Mad2 siRNA) or four cells (control siRNA and EGFP-Kif18A). The average anaphase A velocities in Kif18A-depleted, Kif18A/Mad2-codepleted, and EGFP-Kif18A-expressing cells are significantly different from anaphase A velocities in control cells ($p = 4.9 \times 10^{-9}$, $p = 4.0 \times 10^{-3}$, and $p = 4.4 \times 10^{-16}$, respectively). Anaphase A velocities in Mad2-depleted and Kif18A/Mad2-codepleted cells are also significantly different ($p = 0.01$).

Immunofluorescence, Deconvolution, and Linear Protein Mapping

HeLa cells were fixed as previously described (Maney et al., 1998). For drug treatments, cells were treated with 20 μM nocodazole (Sigma), 10 μM vinblastine (Sigma), or an equal volume of DMSO (Sigma) for 30 min prior to fixation. Antibodies against the C terminus of Kif18A were raised in rabbits against a GST-tagged polypeptide containing amino acids 593–898 of Kif18A and then affinity purified. Cells were labeled with the following primary antibodies: mouse-anti-Hec1 (1:500; Abcam), rabbit-anti-Kif18A (1:50), mouse-anti-α-tubulin (1:50; Sigma), or human-CREST serum (1:50; a kind gift from Bill Brinkley) for 1 hr at room temperature. Anti-mouse, anti-rabbit, and anti-human
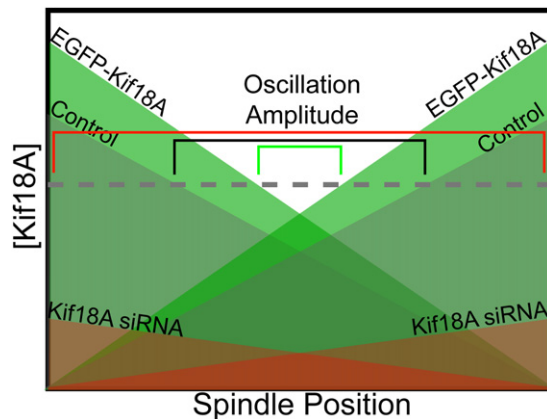
Figure 6. Model for Kif18A Regulation of Mitotic Chromosome Movements

The concentration of Kif18A at kinetochores is proportional to kMT length and stability. Once Kif18A reaches a threshold level (dashed gray line) at kMT plus-ends, it increases the probability that the kMT will undergo catastrophe and therefore increases the probability that the kinetochore will change direction. In a control cell (gray diagonal lines), Kif18A restricts oscillatory movements to a region near the spindle equator where kMTs emanating from opposite poles are of relatively equal length (black bracket). Increasing the concentration of Kif18A in the cell by overexpressing EGFP-Kif18A (green diagonal lines) increases the accumulation of Kif18A on kMTs and further restricts movements (green bracket). Reducing the concentration of Kif18A by treating cells with Kif18A-specific siRNAs (red diagonal lines) prevents threshold accumulation of the motor and leads to larger kinetochore oscillations (red bracket).

secondary antibodies conjugated to fluorescein or rhodamine (Jackson Laboratories) were used at 1:50 for 1 hr at room temperature. Stained cells were mounted in Vectashield with DAPI (Vector). Cells were imaged on a Nikon upright microscope equipped with a CCD camera and a 60× 1.4 NA lens (Nikon) or a Deltavision system equipped with a CCD camera and a 60× 1.4 NA lens (Olympus). Selected images were deconvolved using a Deltavision image-processing workstation (Applied Precision). The linescan function in the Softworx program (Applied Precision) was used to determine the spatial relationships and peak fluorescent values of Hec1 and Kif18A from immunofluorescent images.

SDS-PAGE and Western Blot

HeLa cells were lysed in 1× Laemmli sample buffer 24 or 48 hr after addition of siRNA. Lysates were briefly sonicated, boiled for 10 min, and separated on 4%–12% acrylamide gradient gels by SDS-PAGE. Proteins were transferred to nitrocellulose membrane and analyzed by western blot with polyclonal anti-Kif18A antibodies (1:100) and monoclonal anti-GAPDH antibodies (1:1000; Calbiochem). Proteins were visualized by chemiluminescence, and GAPDH signals were quantified with the gel analyzer function in ImageJ (NIH).

Live Cell Imaging

HeLa cells were cultured in MEMalpha (Life Technologies) medium with 10% FBS (Hyclone) at 37°C and 5% CO_2 on 35 mm^2 glass coverslip dishes coated with poly-l-lysine (MatTek) for 48 hr after DNA transfection and 24–36 hr after siRNA transfection before analysis by time-lapse microscopy. Prior to filming, the cells were switched to 37°C CO_2-independent media (Life Technologies). Cells were imaged with a Deltavision RT system (Applied Precision) equipped with a CCD camera and a 60× 1.42 NA lens (Olympus) and a 37°C environmental chamber (Applied Precision). Z stacks containing five focal planes with 0.5 μm spacing were acquired at intervals of 2, 5, or 20 s. Some cells were also imaged using a CARV (BD Biosciences) spinning-disc confocal system attached to a TE2000 inverted microscope (Nikon) equipped with an ORCA ER (Hamamatsu) camera and a Plan Apo 60× 1.4 NA lens (Nikon).

CARV images were collected at 5 s intervals using a single focal plane. Cells were maintained at 37°C with a thermoelectric stage.

Quantification of Kinetochore Movements

Based on the similarities between kinetochore movements in Kif18A-depleted and EGFP-Kif18A-expressing cells to those of late prometaphase and metaphase control cells, kinetochore movements during these stages in controls were quantified. For all preanaphase measurements, the chosen kinetochores were bioriented, under tension and moving around the equator of the spindle. Kinetochore and spindle pole movements were tracked using maximum-intensity projection movies from live cell imaging experiments and the manual tracking plug-in for ImageJ (NIH). Kinetochore movement parameters, spindle lengths, and interkinetochore distances were quantified from tracking data using Igor Pro 6.0 software (Wavemetrics). All velocity measurements were made by linear regression analysis of kinetochore distance versus time plots. Velocity measurements during oscillatory movements were only made from cells filmed at time intervals of 5 or 2 s because kinetochores filmed at 20 s intervals frequently changed directions between data points, making velocity measurements artifactually low (kinetochores change directions approximately every 40 s in HeLa cells based on our switch rate measurements). Average oscillation amplitudes were calculated by dividing average velocities by average switch rates. Statistical comparisons between data sets were performed using two-tailed t tests assuming unequal variances. In cases where multiple measurements were made from the same kinetochore over time, an average value was calculated. The reported p values are from comparisons of these kinetochore averages, where the number of events is taken as the number of kinetochores analyzed. Indications of significance ($p \leq 0.05$) from statistical tests using average values from each cell analyzed were consistent with those reported, with the exception of interkinetochore distance changes in Kif18A-depleted or EGFP-Kif18A cells, which were not significantly different when compared in this manner.

Supplemental Data

Supplemental Data include four figures and eight movies and are available at http://www.developmentalcell.com/cgi/content/full/14/2/252/DC1/.

REFERENCES

Ault, J.G., DeMarco, A.J., Salmon, E.D., and Rieder, C.L. (1991). Studies on the ejection properties of asters: astral microtubule turnover influences the oscillatory behavior and positioning of mono-oriented chromosomes. J. Cell Sci. *99*, 701–710.

Brinkley, B.R., Zinkowski, R.P., Mollon, W.L., Davis, F.M., Pisegna, M.A., Pershouse, M., and Rao, P.N. (1988). Movement and segregation of kinetochores experimentally detached from mammalian chromosomes. Nature *336*, 251–254.

Buster, D.W., Zhang, D., and Sharp, D.J. (2007). Poleward tubulin flux in spindles: regulation and function in mitotic cells. Mol. Biol. Cell *18*, 3094–3104.

Campbell, R.E., Tour, O., Palmer, A.E., Steinbach, P.A., Baird, G.S., Zacharias, D.A., and Tsien, R.Y. (2002). A monomeric red fluorescent protein. Proc. Natl. Acad. Sci. USA *99*, 7877–7882.

Canman, J.C., Salmon, E.D., and Fang, G. (2002). Inducing precocious anaphase in cultured mammalian cells. Cell Motil. Cytoskeleton *52*, 61–65.

Cassimeris, L., Rieder, C.L., and Salmon, E.D. (1994). Microtubule assembly and kinetochore directional instability in vertebrate monopolar spindles: implications for the mechanism of chromosome congression. J. Cell Sci. *107*, 285–297.

Cimini, D., Moree, B., Canman, J.C., and Salmon, E.D. (2003). Merotelic kinetochore orientation occurs frequently during early mitosis in mammalian tissue cells and error correction is achieved by two different mechanisms. J. Cell Sci. *116*, 4213–4225.

Cimini, D., Cameron, L.A., and Salmon, E.D. (2004). Anaphase spindle mechanics prevent mis-segregation of merotelically oriented chromosomes. Curr. Biol. *14*, 2149–2155.

Gandhi, R., Bonaccorsi, S., Wentworth, D., Doxsey, S., Gatti, M., and Pereira, A. (2004). The *Drosophila* kinesin-like protein KLP67A is essential for mitotic and male meiotic spindle assembly. Mol. Biol. Cell *15*, 121–131.

Ganem, N.J., and Compton, D.A. (2006). Functional roles of poleward microtubule flux during mitosis. Cell Cycle *5*, 481–485.

Ganem, N.J., Upton, K., and Compton, D.A. (2005). Efficient mitosis in human cells lacking poleward microtubule flux. Curr. Biol. *15*, 1827–1832.

Garcia, M.A., Koonrugsa, N., and Toda, T. (2002). Two kinesin-like Kin I family proteins in fission yeast regulate the establishment of metaphase and the onset of anaphase A. Curr. Biol. *12*, 610–621.

Goshima, G., and Vale, R.D. (2003). The roles of microtubule-based motor proteins in mitosis: comprehensive RNAi analysis in the *Drosophila* S2 cell line. J. Cell Biol. *162*, 1003–1016.

Gupta, M.L., Jr., Carvalho, P., Roof, D.M., and Pellman, D. (2006). Plus end-specific depolymerase activity of Kip3, a kinesin-8 protein, explains its role in positioning the yeast mitotic spindle. Nat. Cell Biol. *8*, 913–923.

Inoue, S., and Salmon, E.D. (1995). Force generation by microtubule assembly/disassembly in mitosis and related movements. Mol. Biol. Cell *6*, 1619–1640.

Joglekar, A.P., and Hunt, A.J. (2002). A simple, mechanistic model for directional instability during mitotic chromosome movements. Biophys. J. *83*, 42–58.

Kapoor, T.M., and Compton, D.A. (2002). Searching for the middle ground: mechanisms of chromosome alignment during mitosis. J. Cell Biol. *157*, 551–556.

Khodjakov, A., Gabashvili, I.S., and Rieder, C.L. (1999). "Dumb" versus "smart" kinetochore models for chromosome congression during mitosis in vertebrate somatic cells. Cell Motil. Cytoskeleton *43*, 179–185.

Levesque, A.A., and Compton, D.A. (2001). The chromokinesin Kid is necessary for chromosome arm orientation and oscillation, but not congression, on mitotic spindles. J. Cell Biol. *154*, 1135–1146.

Maddox, P.S., Bloom, K.S., and Salmon, E.D. (2000). The polarity and dynamics of microtubule assembly in the budding yeast *Saccharomyces cerevisiae*. Nat. Cell Biol. *2*, 36–41.

Mallavarapu, A., Sawin, K., and Mitchison, T. (1999). A switch in microtubule dynamics at the onset of anaphase B in the mitotic spindle of *Schizosaccharomyces pombe*. Curr. Biol. *9*, 1423–1426.

Maney, T., Hunter, A.W., Wagenbach, M., and Wordeman, L. (1998). Mitotic centromere-associated kinesin is important for anaphase chromosome segregation. J. Cell Biol. *142*, 787–801.

Mayr, M.I., Hümmer, S., Bormann, J., Grüner, T., Adio, S., Woehlke, G., and Mayer, T.U. (2007). The human kinesin Kif18A is a motile microtubule depolymerase essential for chromosome congression. Curr. Biol. *17*, 488–498.

Meraldi, P., Draviam, V.M., and Sorger, P.K. (2004). Timing and checkpoints in the regulation of mitotic progression. Dev. Cell *7*, 45–60.

Mitchison, T.J. (1989). Chromosome alignment at mitotic metaphase: balanced forces or smart kinetochores? In Cell Movement, Volume 2: Kinesin, Dynein and Microtubule Dynamics, D.F. Warner and J.R. McIntosh, eds. (New York: Alan R. Liss), pp. 421–430.

Moore, A.T., Rankin, K.E., von Dassow, G., Peris, L., Wagenbach, M., Ovechkina, Y., Andrieux, A., Job, D., and Wordeman, L. (2005). MCAK associates with the tips of polymerizing microtubules. J. Cell Biol. *169*, 391–397.

Pearson, C.G., Maddox, P.S., Zarzar, T.R., Salmon, E.D., and Bloom, K. (2003). Yeast kinetochores do not stabilize Stu2p-dependent spindle microtubule dynamics. Mol. Biol. Cell *14*, 4181–4195.

Pereira, A.J., Dalby, B., Stewart, R.J., Doxsey, S.J., and Goldstein, L.S. (1997). Mitochondrial association of a plus end-directed microtubule motor expressed during mitosis in *Drosophila*. J. Cell Biol. *136*, 1081–1090.

Rieder, C.L., and Salmon, E.D. (1994). Motile kinetochores and polar ejection forces dictate chromosome position on the vertebrate mitotic spindle. J. Cell Biol. *124*, 223–233.

Rieder, C.L., Davison, E.A., Jensen, L.C., Cassimeris, L., and Salmon, E.D. (1986). Oscillatory movements of monooriented chromosomes and their position relative to the spindle pole result from the ejection properties of the aster and half-spindle. J. Cell Biol. *103*, 581–591.

Skibbens, R.V., Skeen, V.P., and Salmon, E.D. (1993). Directional instability of kinetochore motility during chromosome congression and segregation in mitotic newt lung cells: a push-pull mechanism. J. Cell Biol. *122*, 859–875.

Varga, V., Helenius, J., Tanaka, K., Hyman, A.A., Tanaka, T.U., and Howard, J. (2006). Yeast kinesin-8 depolymerizes microtubules in a length-dependent manner. Nat. Cell Biol. *8*, 957–962.

West, R.R., Malmstrom, T., and McIntosh, J.R. (2002). Kinesins klp5(+) and klp6(+) are required for normal chromosome movement in mitosis. J. Cell Sci. *115*, 931–940.

Woehlke, G., Ruby, A.K., Hart, C.L., Ly, B., Hom-Booher, N., and Vale, R.D. (1997). Microtubule interaction site of the kinesin motor. Cell *90*, 207–216.

Zhu, C., Zhao, J., Bibikova, M., Leverson, J.D., Bossy-Wetzel, E., Fan, J.B., Abraham, R.T., and Jiang, W. (2005). Functional analysis of human microtubule-based motor proteins, the kinesins and dyneins, in mitosis/cytokinesis using RNA interference. Mol. Biol. Cell *16*, 3187–3199.

Developmental Cell *14*

Supplemental Data

The Kinesin-8 Motor Kif18A Suppresses Kinetochore

Movements to Control Mitotic Chromosome Alignment

Jason Stumpff, George von Dassow, Michael Wagenbach, Charles Asbury, and Linda Wordeman
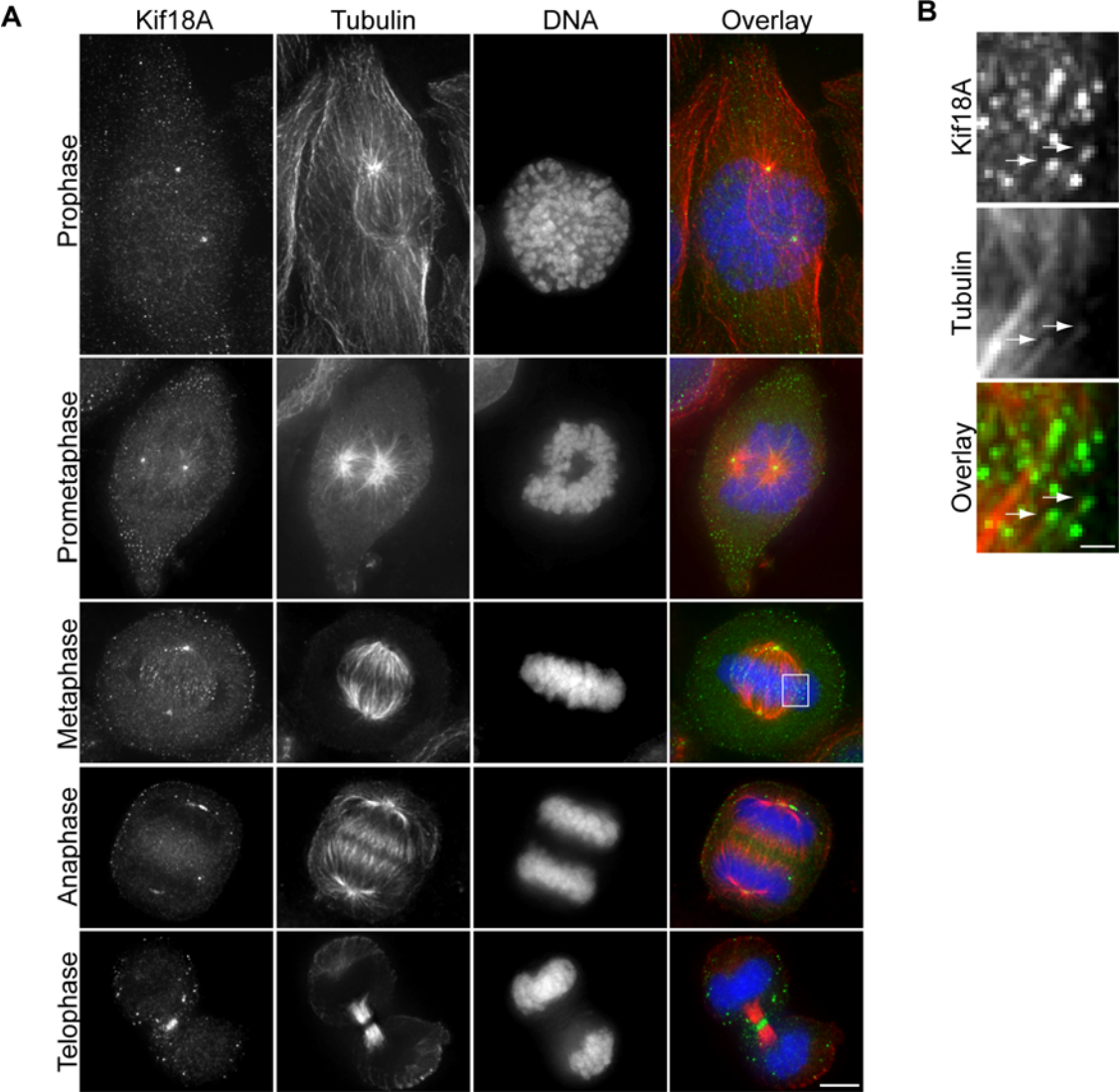

Figure S1. Kif18A Localizes Dynamically to the Plus-Ends of Kinetochore

Microtubules during Mitosis

(A) Mitotic HeLa cells in the indicated stages were fixed and stained with anti-Kif18A antibodies (green in overlay), anti-α-tubulin antibodies (red in overlay), and DAPI to visualize DNA (blue in overlay).

(B) Magnified view of the region indicated by the white box in the metaphase cell in (A). White arrows indicate kMTs with visible gradients of Kif18A.
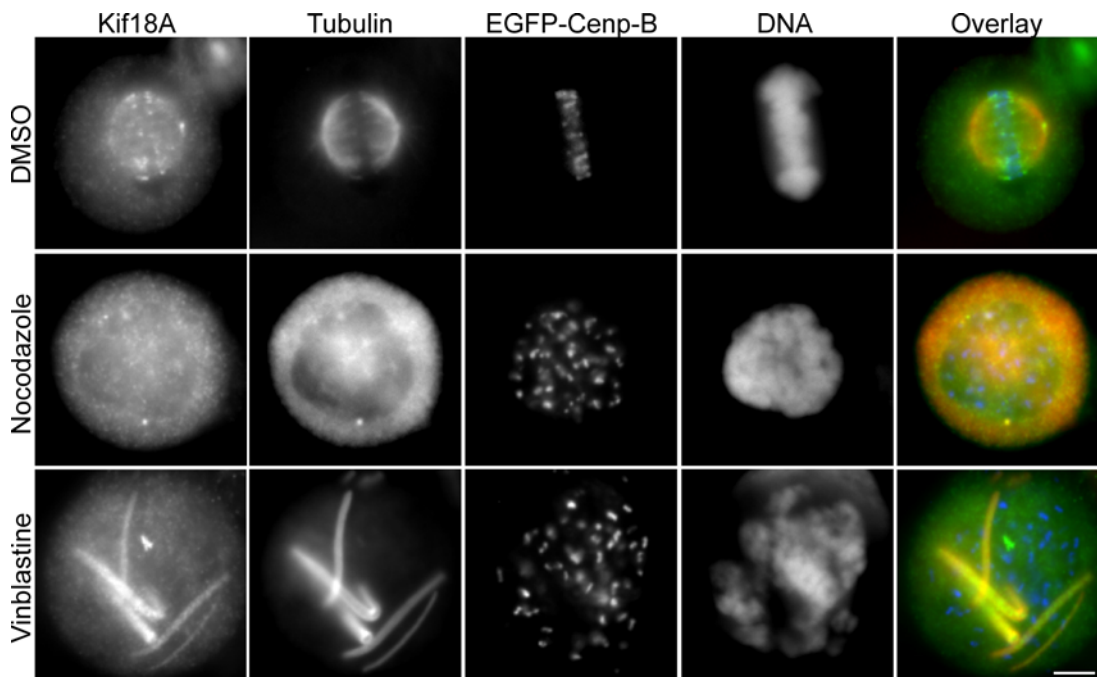

Figure S2. Localization of Kif18A to Kinetochores Is Dependent on Microtubules

HeLa cells expressing EGFP-CENP-B (blue in overlay) were treated with the indicated drugs for 30 minutes prior to fixation and staining with anti-Kif18A antibodies (green in overlay), anti-α-tubulin antibodies (red in overlay) and DAPI to visualize DNA.
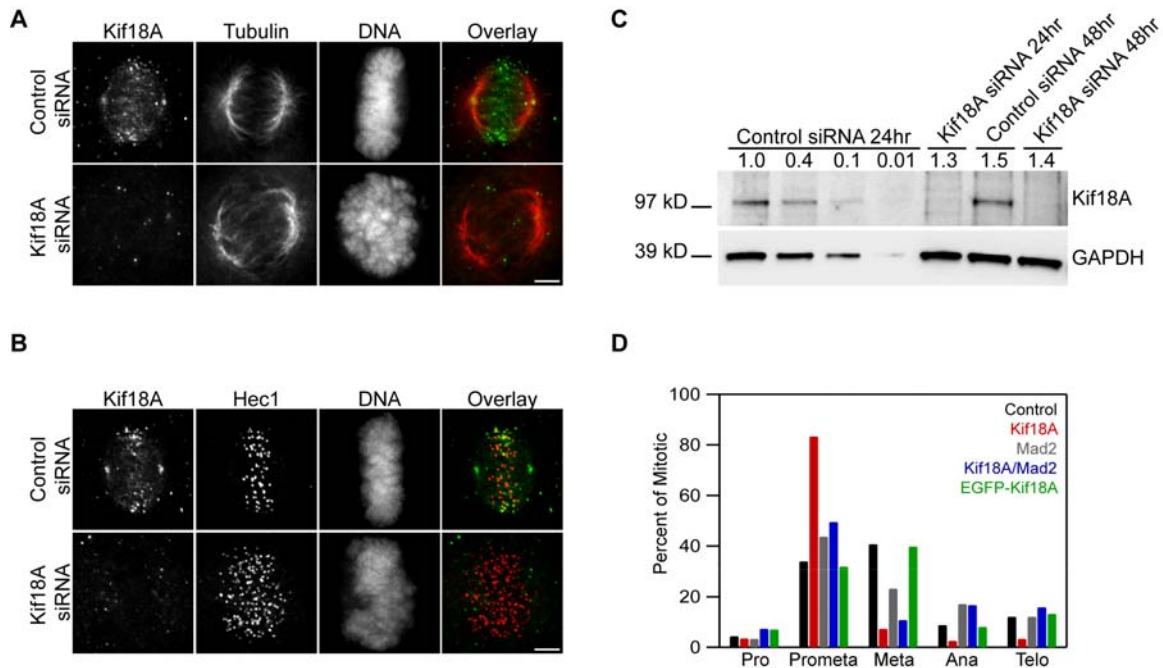
Figure S3. Treatment with Kif18A-Specific siRNAs Depletes Kif18A from Spindles and Delays Cells in Prometaphase

(A and B) HeLa cells were treated with control or Kif18A-specific siRNA for 36 hours prior to fixation and staining with anti-Kif18A antibodies (green in overlay), anti-α-tubulin antibodies (red in overlay in (A)), anti-Hec1 antibodies (red in overlay in (B)) and DAPI to visualize DNA. Scale bars are 5 μm.

(C) Western blot analysis of Kif18A in HeLa cell extracts after treatment with control or Kif18A-specific siRNAs for 24 or 48 hours as indicated. The numbers above each lane indicate the relative abundance of the GAPDH loading control.

(D) HeLa cells were transfected with control (black bars), Kif18A-specific (red bars), Mad2-specific (blue bars) or a combination of Kif18A and Mad2-specific siRNAs (gray bars) 24 hours prior to fixation or EGFP-Kif18A (green bars) 48 hours prior to fixation. The percentage of mitotic cells in prophase (Pro), prometaphase (Promet), metaphase (Meta), anaphase (Ana) and telophase

(Telo) were then quantified for each population of cells using DNA and tubulin staining to determine mitotic stages. Percentages were averaged from two separate experiments. The total number of mitotic cells scored was 297 (control siRNA), 462 (Kif18A siRNA), 277 (Mad2 siRNA), 274 (Kif18A and Mad2 siRNA) and 260 (EGFP-Kif18A).
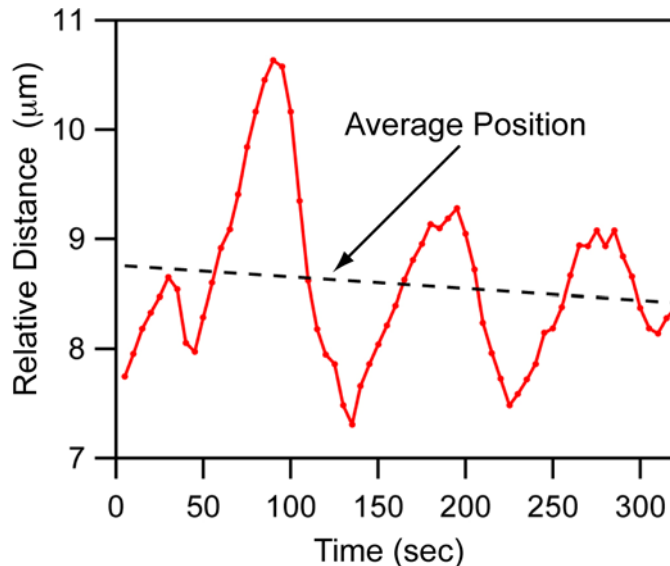

Figure S4. Deviation from Average Position (DAP) Measurements

Previous studies have established methods for quantifying mitotic kinetochore dynamics that involve measuring velocities and switch frequencies during intervals of poleward and away-from-pole movement. While these methods provide detailed information about kinetochore movements, their use is limited to cases where reversals in direction can be unambiguously scored. In some cases (e.g. Kif18A overexpression) directional switches are not readily apparent, precluding this type of analysis. Therefore we developed an alternative method for quantifying the magnitude of oscillatory movements, based on the deviations that a kinetochore makes from its average position. This method has the

advantage that it does not require hand-selection of directional changes. Therefore it avoids subjectivity and can be applied in cases where turnarounds are not apparent.

To define the average position for a kinetochore, a regression line (dashed black line) was fit to a position versus time plot of the kinetochore's movement relative to spindle pole position (red line and points). The distance between the kinetochore and the fit-line was measured at each time point and the standard deviation of those distances was defined as the deviation from average position (DAP). In cases where experimental treatments do not change the basic shape of the distance versus time plots (for example by significantly increasing pauses in movement), DAP provides a linear measurement of oscillation amplitude that is sensitive to changes in kinetochore oscillation frequency and velocity. In both control and Kif18A-depleted HeLa cells, DAP values are approximately 38% of the average oscillation amplitude.